Food Chemistry 115 (2009) 1529–1541

Contents lists available at ScienceDirect

Food Chemistry

journal homepage: www.elsevier.com/locate/foodchem

Analytical Methods

On-line separation and structural characterisation of feruloylated oligosaccharides from wheat bran using HPLC-ESI-MS^n

Jing Wang [a,*], Xiaoping Yuan [b], Baoguo Sun [a], Yanping Cao [a], Yuan Tian [a], Chengtao Wang [a]

[a] College of Chemistry and Environment Engineering, Beijing Technology and Business University, 11 Fucheng Road, Beijing 100048, PR China
[b] Department of Science and Technology, China Grain Reserves Corporation, 143A, Xizhimenwai Street, Beijing 100044, P.R. China

ARTICLE INFO

Article history:
Received 25 August 2008
Received in revised form 6 December 2008
Accepted 21 January 2009

Keywords:
ESI-MS^n
Feruloylated oligosaccharides
HPLC
Wheat bran

ABSTRACT

Water-soluble feruloylated oligosaccharides (FOs) from wheat bran, ferulic acid esters of arabinoxylan oligosaccharides, have been reported as natural antioxidants. In this study, structure features of FOs were studied by FT-IR spectroscopy, and high-performance liquid chromatography (HPLC) coupled to electrospray ionisation (ESI) mass spectrometry (MS) was used for separation and characterisation of FOs. Four components of FOs were resolved on a Dikma Technologies Diamonsil™ C_{18} column eluted with water/acetonitrite (90:10) containing 0.5% HCOOH (V/V) and further analysed by ESI-MS^n. In ESI-MS^n, a predominant $[M+NH_4]^+$ ion in positive mode and $[M-H]^-$ ion in negative mode were observed for molecular mass information. The ESI-MS^n spectra of the deprotonated molecular $[M-H]^-$ ion were used for structural elucidation. The structures of four isolated compounds were confirmed for the first time by on-line HPLC-ESI-MS^n.

1. Introduction

Hemicellulose is one of the main polysaccharides of the cell wall in higher plants. In cereals, the hemicellulose fraction is composed mainly of arabinoxylans. Arabinoxylans, the predominant nonstarch polysaccharides from cell walls of cereal endosperm, are complex, highly heterogeneous polysaccharides, consisting of a linear β-(1,4) linked xylopyranose backbone to which α-L-arabinofuranose units are attached *via* α-(1,3) and/or α-(1,2) linkages. A feature of some arabinoxylans is the existence of feruloyl residues that are covalently bound to arabinosyl side chains of xylans *via* ester bonds (Lequart, Nuzillard, Kurek, & Debeire, 1999).

Many studies have been performed for isolation of feruloylated oligosaccharides (FOs) from Gramineae by mild acid hydrolysis or by treatment with a mixture of polysaccharide hydrolysing enzymes (Ishii, 1997). Isolation of these FOs has allowed a better understanding of the plant cell wall structures. FOs prepared so far from graminaceous cell walls have shown good consistency of structure. The α-L-arabinofuranosyl residues are attached to *O*-3 positions of β-1,4-linked D-xylan and are substituted at position *O*-5 with a feruloyl group (Yoshida-Shimokawa, Yoshida, Kakegawa, & Ishii, 2001). Furthermore, interest in these oligosaccharides is motivated by their biological activities and their technological applications. FOs possess *in vitro* antioxidant activity against free radical-induced oxidative damage in normal rat erythrocytes, and stimulate *in vitro* growth of *Bifidobacterium bifidum* (Yuan, Wang, Yao, & Chen, 2005; Yuan, Wang, & Yao, 2005). More interestingly, antioxidative activities of FOs were stronger than that of free ferulic acid in a microsomal lipid peroxidation system and a low density lipoproteins oxidation system (Ohta, Yamasaki, Egashira, & Sanada, 1994; Katapodis et al., 2003). In an *in vivo* study, FOs are a suitable antioxidant for protection against oxidative damage in diabetic rats (Ou et al., 2007).

Many studies involving the structural characterisation of FOs have been done mainly by nuclear magnetic resonance (NMR) (Smith & Hartley, 1983; Lequart et al., 1999; Rhodes, Sadek, & Stone, 2002). However, prior to analysis using NMR, purification of the oligosaccharides is needed and this procedure is time-consuming, and sometimes, it is very difficult to obtain the relatively large amounts of a required sample with a high degree of purity. On the other hand, electrospray ionisation multi-stage tandem mass spectrometry (ESI-MS^n), and HPLC-ESI-MS^n have gained increasing importance as detection methods for oligosaccharide analysis and characterisation (Saad & Leary, 2005; Geng, Qiu, Zhu, & Bai, 2008). ESI has been recognised as a powerful ionisation technique for the introduction of oligosaccharides into an MS. Development of the MS–MS technique enables one to get the product ion spectrum from a parent ion and to obtain considerable structural information about the corresponding components. Its main advantage over NMR spectroscopy is the low detection limit, which makes detection of heterogeneity easier. A variety of thermolabile, polar and nonvolatile compounds present in a complex matrix can be separated, characterised and quantified unambiguously. Recently, negative- and positive-ion electrospray mass spectrometry were successfully applied to the structural characterisation of underivatised arabino-xylo-oligosaccharides and feruloylated arabino-oligosaccharides (Quéméner, Ordaz-Ortiz, & Saulnier, 2006; Vafiadi, Topakas,

* Corresponding author. Tel.: +86 10 68985378; fax: +86 10 68985456.
E-mail address: jingw810@yahoo.com (J. Wang).

0308-8146/$ - see front matter © 2009 Elsevier Ltd. All rights reserved.
doi:10.1016/j.foodchem.2009.01.058

Bakx, Schols, & Christakopoulos, 2007). Several HPLC-ESI-MS^n studies have been performed on underivatised or derivatised oligosaccharides and glycosides (Liu, Urgaonkar, Verkade, & Armstrong, 2005; Broberg, 2007; Bonaccorsi, Caristi, Gargiulli, & Leuzzi, 2008). However, to the best of our knowledge, few systematic studies on fragmentation behaviours of wheat bran FOs by HPLC-ESI-MS^n have been reported. In the presented paper, the structural characterisation of wheat bran FOs was elucidated for the first time by Fourier transform infrared (FT-IR) spectrum and on-line HPLC-ESI-MS^n.

2. Materials and methods

2.1. Materials

FOs were supplied by Dr. Xiaoping Yuan. Acetonitrile was of MS grade and all other reagents were of HPLC grade and purchased from Sigma–Aldrich (St. Louis, MO).

2.2. Equipments

Fourier-transform infrared (FT-IR) spectra were obtained using a Nicolet Nexus FT-IR spectrophotometer (Thermo Electron Corporation, Waltham, MA) equipped with an OMNI-Sampler, a deuterated triglycine sulphate (DTGS) detector, a Ge-on KBr beam splitter (7800–350 cm^{-1}), a Smart Diffuse Reflection accessory, a single reflection horizontal attenuated total reflection (ATR) attachment and OMNIC 6.2 software. The spectrum was taken with a resolution of 4 cm^{-1} and accumulation of 64 scans.

Liquid chromatography and mass spectrometry (LC/MS) were carried out using a system equipped with Surveyor LC system (Thermo Finnigan, San Jose, CA) including quaternary pump, on-line degasser, column heater compartment, autosampler and photodiode array detector (PDA), and an LCQ DECA XP^{plus} mass spectrometer (Thermo Finnigan) that consists of an ESI interface and an ion-trap mass analyser. The software for the control of the equipment, and the acquisition and treatment of data is the Xcalibur 1.3 Workstation.

2.3. FT-IR spectroscopy

An FT-IR spectrum of FOs was collected between 4000 and 500 cm^{-1} (mid-infrared region) on a Nicolet Nexus FT-IR spectrophotometer with 256 scans at a resolution of 4 cm^{-1}. The sample was ground with spectroscopic grade potassium bromide (KBr) powder and then pressed into 1 mm pellets (2 mg of sample per 200 mg dry KBr). A blank KBr disk was used as background. The FT-IR spectrum was smoothed and the baseline was corrected automatically using the built-in software of the spectrophotometer (OMNIC 3.2).

2.4. On-line HPLC-ESI-MS^n

FOs were dissolved in 50% methanol (v/v) and then ultrafiltered before HPLC analysis. HPLC separation was performed on a Dikma Technologies Diamonsil^{TM} C_{18} column (4.6 × 250 mm, 5 μm particle size, Dikma, Beijing, China). A volume of 20 μl of the sample solution of FOs was injected into the HPLC column. The column was maintained at 25 °C and eluted with water/acetonitrile (90:10) containing 0.5% HCOOH (v/v) at a flow rate of 1 ml/min. The absorbance of the eluate was monitored continuously at 325 nm with a PDA.

The elution from the HPLC was passed through the PDA and then directly introduced into the mass spectrometry using electrospray ionisation (ESI). All the analyses were performed using the ESI interface with the following settings: negative ionisation mode; temperature of the capillary, 300 °C, spray voltage, 4.0 kV; capillary voltage, −15 V; sheaht gas (N_2) flow, 20 A.U.; auxiliary gas (N_2) flow, 10 A.U. For MS^n experiments, the various parameters were adjusted for the tested sample to optimise signal and get maximal structural information from the ion of interest.

3. Results and discussion

The tested FOs in this study were prepared from wheat bran insoluble dietary fibre by *Bacillus subtilis* xylanase treatments. FOs by treatment with NaOH released ferulic acid and arabinoxylan oligosaccharides which consisted of arabinose and xylose (Yuan et al., 2005). Smith and Hartley (1983) reported a feruloyl arabinoxylan disaccharide, 2-*O*-[5-*O*-(*trans*-feruloyl)-α-L-arabinofuranosyl]-D-xylopyranose, was isolated from the *Oxyporus* cellulase digest of cell walls of wheat bran. An *O*-[5-*O*-feruloyl-α-L-arabinofuranosyl]-(1,3)-*O*-β-D-xylopyranosyl-(1,4)-β-D-xylopyranose, an *O*-β-D-xylopyranosyl-(1,4)-*O*-[5-*O*-feruloyl-α-L-arabinofuranosyl-(1,3)]-*O*-β-D-xylopyranosyl-(1,4)-D-xylopyranose, an *O*-β-D-xylopyranosyl–(1,4)-*O*-[5-*O*-feruloyl-α-L-arabinofuranosyl-(1,3)]-*O*-β-D-xylo-pyranosyl-(1,4)-*O*-β-D-xylopyranosyl-(1,4)-D-xylopyranose were isolated from the enzymatic hydrolysate of cell walls of wheat bran (McCallum, Taylor, & Neil Towers, 1991; Lequart et al., 1999; Rhodes et al., 2002). The composition of the tested FOs in this study showed good consistency with that of the feruloylated arabinoxylan oligosaccharides above.

3.1. FT-IR spectroscopy of FOs

FT-IR spectroscopy has been proved to be useful for studying physicochemical and conformational properties of carbohydrates. Oligosaccharides have been shown to be suitable models for understanding the conformation in the solid state and in aqueous solution, as well as intermolecular interactions (Kačuráková, Belton, Wilson, Hirsch, & Ebringerová, 1998). In this study, FT-IR spectroscopy was used to evaluate the structural characterisation. The FT-IR spectrum of FOs is shown in Fig. 1. The broad absorbance band at 3600–3200 cm^{-1} is due to stretching of the hydroxyl groups, including carbohydrate and phenolic hydroxyl groups. The absorbance band at 3200–2800 cm^{-1} is attributed to the C–H stretching and bending vibrations. It is noticeable that a small band at 1731 cm^{-1} is due to the ferulic acid ester group of the oligosaccharides, which is supported by these characteristic absorption bands at 1731 and 1253 cm^{-1} (conjugated double bonds), and a phenyl ring group at 1596 cm^{-1} (Dobhal, Hasan, Sharma, & Joshi, 1999). Each particular carbohydrate has a specific band in the 1200–900 cm^{-1} region, which is within the so-called fingerprint region, where the position and the intensity of the bands are specific for each sugar, allowing its possible identification (Kačuráková, Capeka, Sasinková, Wellner, & Ebringerová, 2000). The region is dominated by ring vibrations overlapped with stretching vibration of (C–OH) side groups and the (C–O–C) glycosidic band vibration. A band at 1161 cm^{-1} and the maximum absorption band around 1042 cm^{-1} are typical of xylooligosaccharides. The prominent band at 1042 cm^{-1} is attributed to the C–O, C–C stretching or C–O bending in xylooligosaccharides, which shows variation in spectral shape depending on the branches at the *O*-2 and *O*-3 positions. The changes of the characteristic spectra of xylooligosaccharides in the fingerprint region are associated with the substitution of arabinosyl residues at the *O*-3 position of xylosyl and are accompanied by a decrease in transmittance intensity (1164 and 895 cm^{-1}) and a loss of peak intensity (1120–1000 cm^{-1}) (Nandini & Salimath, 2001). Two low-intensity shoulders at 987 and 1078 cm^{-1} are assigned to an arabinosyl residue attached only at *O*-3 of the xylosyl residues, a characteristic typical of substituted xylooligosaccharides. The sharp

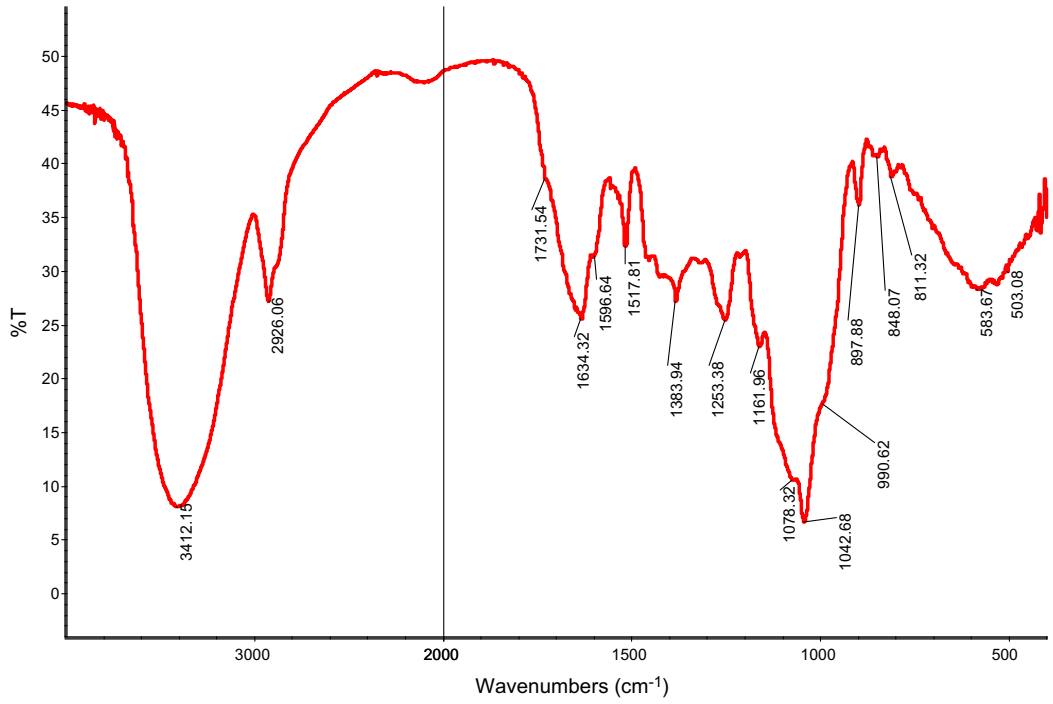

Fig. 1. FT-IR spectrum of wheat bran FOs.

band at 897 cm^{-1} which is attributed to the glycosidic C_1–H deformation with ring vibration contribution and OH bending is characteristic of β-glycosidic linkages between the sugar units (Chaikumpollert, Methacanon, & Suchiva, 2004). This confirmed that the xylopyranose residues forming the backbone of the molecule are linked by β-form bonds. The signal at 1634 cm^{-1} can be attributed to the absorbed water, since xylooligosaccharides usually have a strong affinity for water, and FOs in solid state may have disordered structures which can easily be hydrated. The remaining signals in the spectrum at 1383 and 1253 cm^{-1} relate to C–C and C–O stretching and CH or OH bending in oligosaccharides. The occurrence of a band at 1517 cm^{-1} is largely due to the presence of small amounts of residual lignin. The characteristic absorption at 848 cm^{-1} in the IR spectrum indicates the α-glycosidic linkages of the glycosyl residues. The band near 811 cm^{-1} may be related to β-glycosidic linkages of furanose derivatives (Bahmed, Quilès, Bonaly, & Coulon, 2003). Based on the above mentioned analyses and the compositions of FOs, it is possible to speculate that the backbone of FOs consists of linear β-linked xylopyranosyl residues, and the ararbinofuranosyl residue is attached at *O*-3 position of xylose residues *via* α-form bond, and ferulic acid is bound to the arabinose residue.

3.2. HPLC-ESI-MS of FOs

HPLC chromatography coupled with mass spectrometry is a very powerful analytical technique, due to its high sensitivity, and the structural information that can be obtained about the analytes. The electrospray ionisation interface is very appropriate for the analysis of polar nonvolatile compounds. For example, underivatised oligosaccharides have been separated and characterised by HPLC-ESI-MS (Liu et al., 2005). In this study, FOs was analysed using HPLC-ESI-MS^n. FOs exhibited a maximum UV absorbance at 325 nm due to their ferulic acid moiety. Fig. 2a and b shows the liquid and total ion chromatogram of FOs; four major compounds with the retention time of 11.31, 12.77, 13.53 and 14.81 min, were observed. Under ESI-MS conditions, FOs had strong species both in positive and negative ion modes. The full-scan mass spectra in positive and negative ion modes of compounds **1–4** are shown in Fig. 3. The main peak at *m/z* 872 in Fig. 3a and c was assigned to the ammonium adduct $[M+NH_4]^+$. In negative ion mode shown in Fig. 3b and d, the deprotonated ion $[M-H]^-$ at *m/z* 853 was displayed. By comparing the pair of ions, it is easy to confirm the molecular mass of compounds **1** and **2** as 854 Da. As shown in Fig. 3e and g, the main peak at *m/z* 740 was assigned to the ammonium adduct $[M+NH_4]^+$. In negative ion mode shown in Fig. 3f and h, the deprotonated ion $[M-H]^-$ at *m/z* 721 was displayed. By comparing the pair of ions, it is easy to confirm the molecular mass of compounds **3** and **4** as 722 Da.

Wheat bran arabinoxylans consist of a linear backbone of β-(1,4) linked d-xylopyranosyl residues containing individual α-L-arabinofuranosyl residues attached through *O*-2 and/or *O*-3, and the arabinofuranosyl feruloylated derivative is found at the *O*-3 position of the xylosyl residue (Benamrouche, Crônier, Debeirem, & Chabbertm, 2002). FOs prepared so far from graminaceous cell walls have shown good consistency of structure. The α-L-arabinofuranosyl residues are attached to *O*-3 positions of β-1,4-linked D-xylan and is substituted at position *O*-5 with feruloyl group (Yoshida-Shimokawa et al., 2001). Therefore, based on the composition and ESI-MS analyses of FOs, it is easily speculated that compounds **1** and **2** are feruloyl arabinosyl xylotetraose, compounds **3** and **4** are feruloyl arabinosyl xylotriose.

3.3. ESI-MS^n of FOs

Negative-ion ESI-MS^n provides a sensitive means for structural analysis of neutral underivatised oligosaccharides, due to the low chemical background noise and the low level of cation adduct formation in negative-ion mode (Chai, Piskarev, & Lawson, 2001). The peculiarity of negative ionisation is believed to consist in a selective deprotonation of the anomeric hydroxyl (reducing end of the oligosaccharide chain), which is more acidic, with respect to the remaining OH groups. Once the negative charge is localised at the oligosaccharide reducing end, the ion fragmentation of this ring

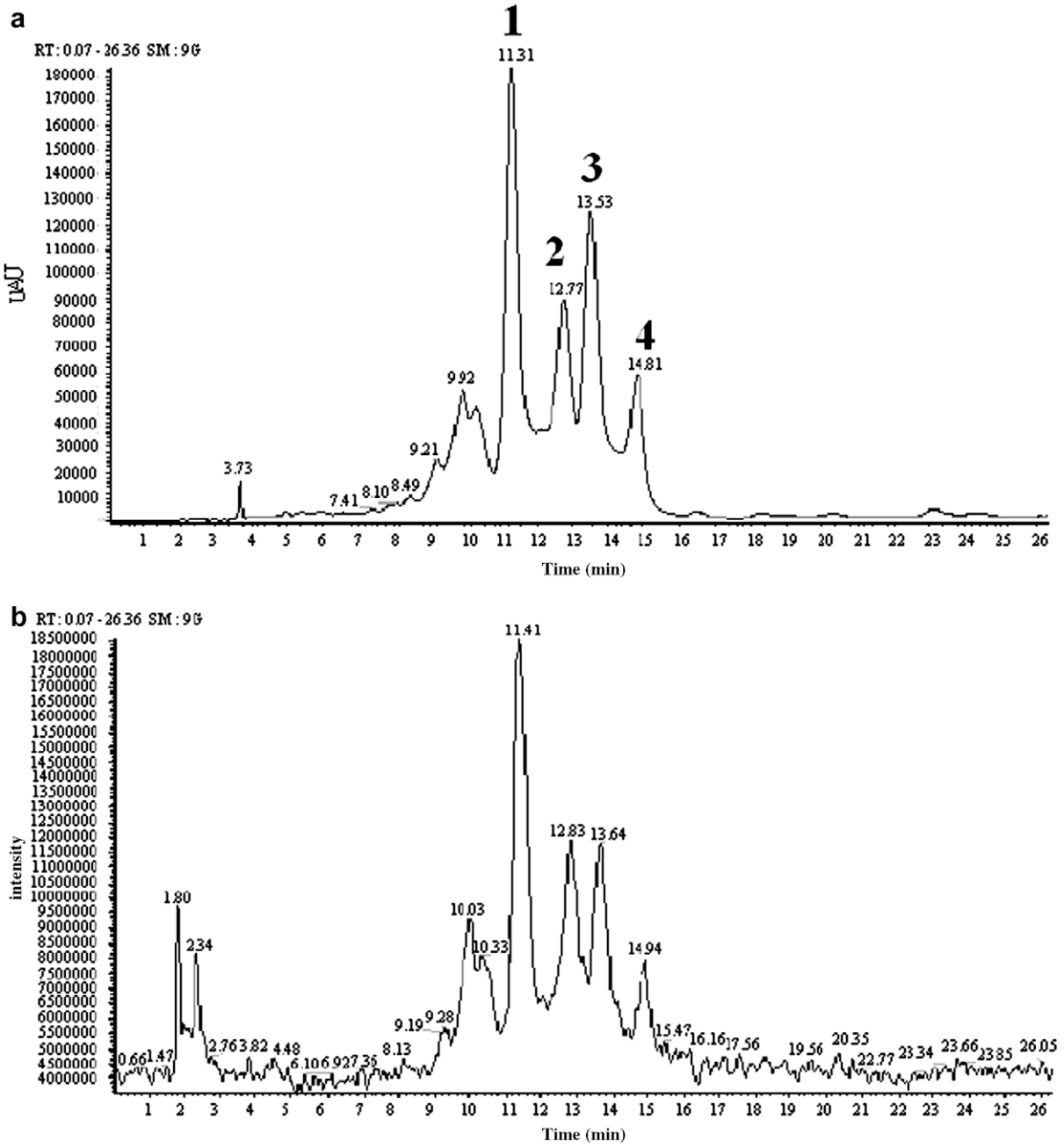

Fig. 2. (a) HPLC-UV chromatogram of FOs and (b) total ion current chromatogram of FOs.

occurs rapidly and the mass losses observed are found to be diagnostic of the glycoside linkage type between adjacent sugar units (Garozzo, Giuffrida, & Impallomeni, 1990). MS^n spectra of deprotonated oligosaccharides can be read "from right to left", paying attention to distinct mass increments (Pfenninger, Karas, Finke, & Stahl, 2002a).

The ESI mass spectra in negative mode involve deprotonated species. Figs. 4–7 show the MS^n spectra of deprotonated molecule $[M-H]^-$ ions at *m/z* 853 of compounds **1** and **2**, and at *m/z* 721 of compounds **3** and **4**. Under negative-ion ESI-MS^n condition, the fragmentation process of oligosaccharides involves the glycosidic cleavage between two sugar residues and cross-ring opening of sugar (cleavage of two bonds within the sugar ring). The fragment ions observed in the MS^n spectra are usually named according to the nomenclature proposed by Domon and Costello (1988), as shown in Fig. 8. Oligosaccharide fragment ions that retain the charge at the carbohydrate portion are designated as A_i, when originated by crossing-ring cleavages, or B_i and C_i when originated by glycosidic cleavage, where *i* represents the number of the glycosidic bond cleaved, counted from the non-reducing end. On the other hand, fragment ions that retain the charge at the reducing end are designated X_j when originated by cross-ring cleavages, or Y_j and Z_j when originated by glycosidic cleavage, where *j* is the number of the interglycosidic bond counted from the aglycone (or the reducing end for carbohydrates). The glycosidic bond linking to aglycone is numbered 0. Following the letter that defines the fragment type, there is a number in superscript that identifies the number of sugar residues in a linear oligosaccharide, or the Greek letters (e.g., α) for branched oligosaccharides in the order of the size of branching.

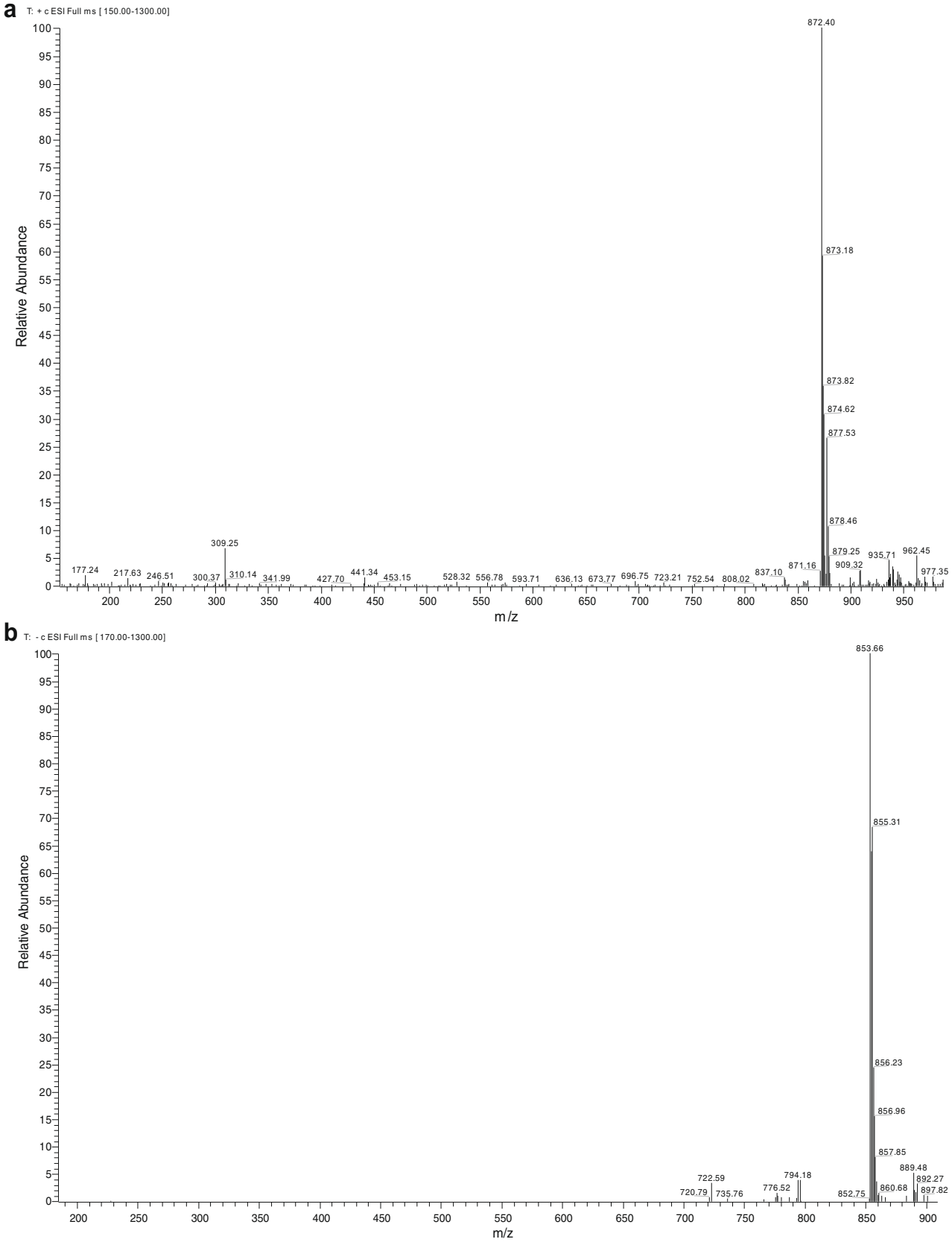

Fig. 3. (a,c,e,g) Positive ion mass spectra of compounds **1**–**4**; (b,d,f,h) Negative ion mass spectra of compounds **1**–**4**.

*3.3.1. Identification of compounds **1** and **2***

Fig. 9a shows the proposed structure of compound **1** and the different cleavages observed. After collision-induced dissociation of the parent ion at *m/z* 853, the glycosidic bond and sugar ring were cleaved to form A and C type fragment ions, including mainly *m/z* 793 ($^{0,2}A_4$), 775, 721 (C_3), 661 ($^{0,2}A_3$), 643, 589 (C_2), 325 ($C_{1\alpha}$),

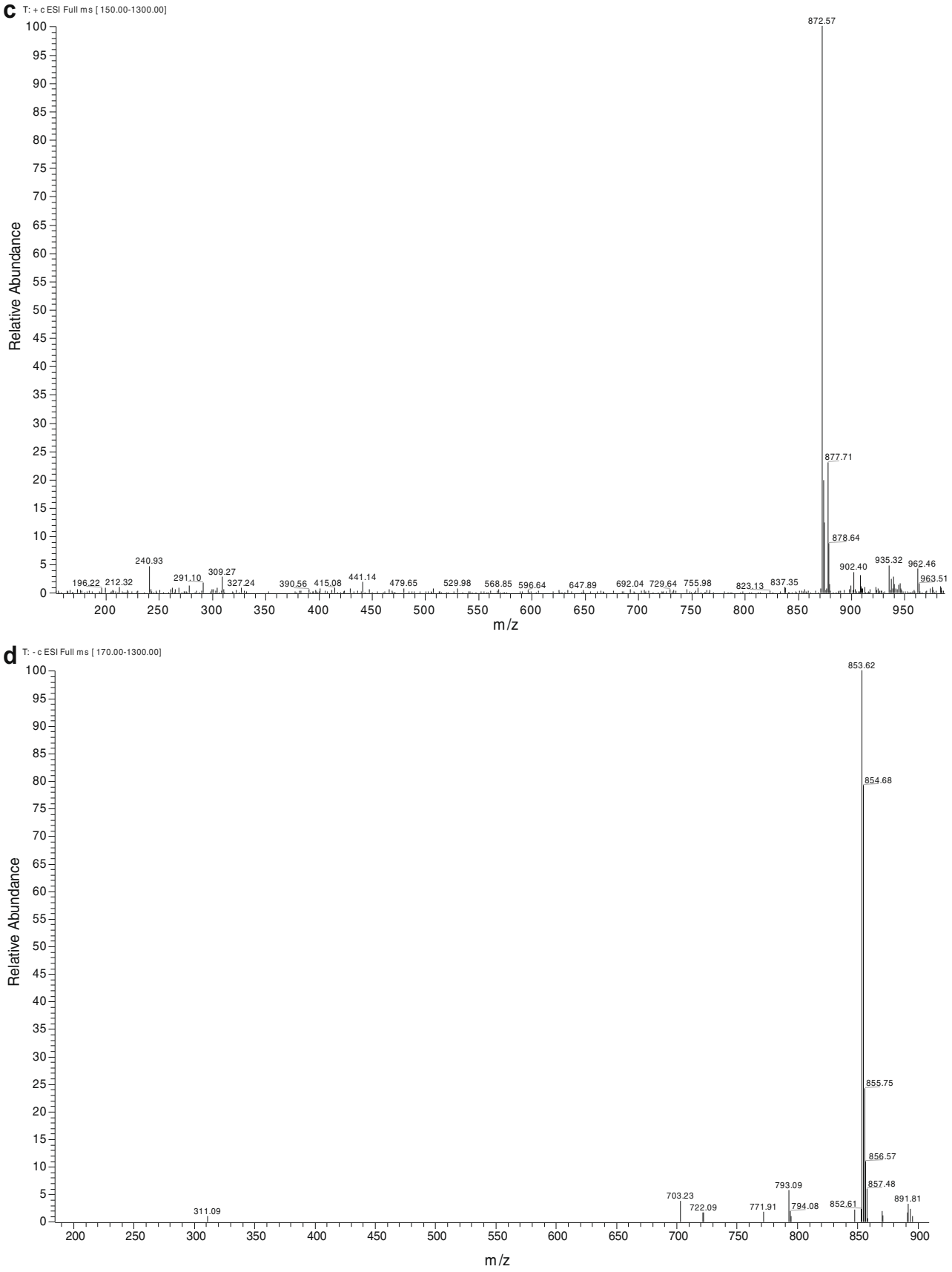

Fig. 3 (*continued*)

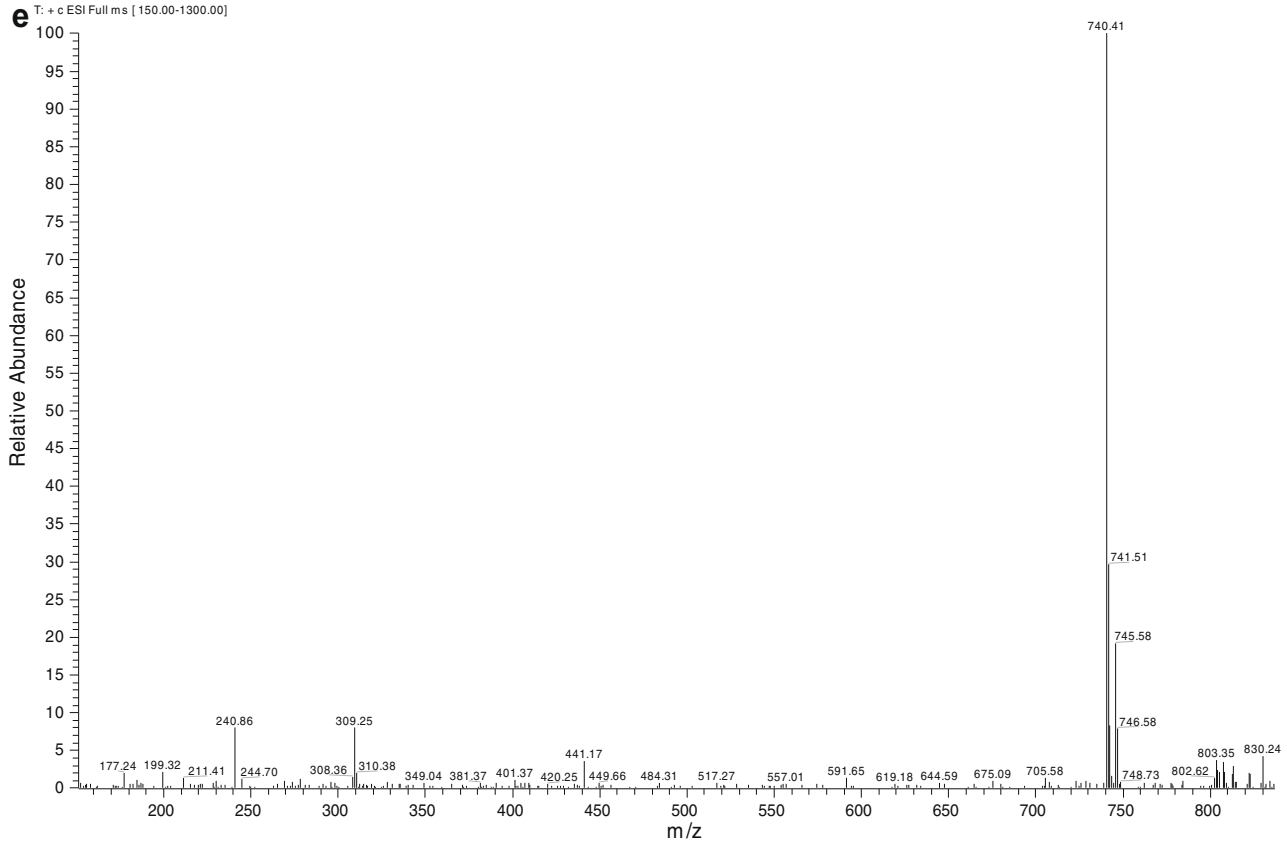

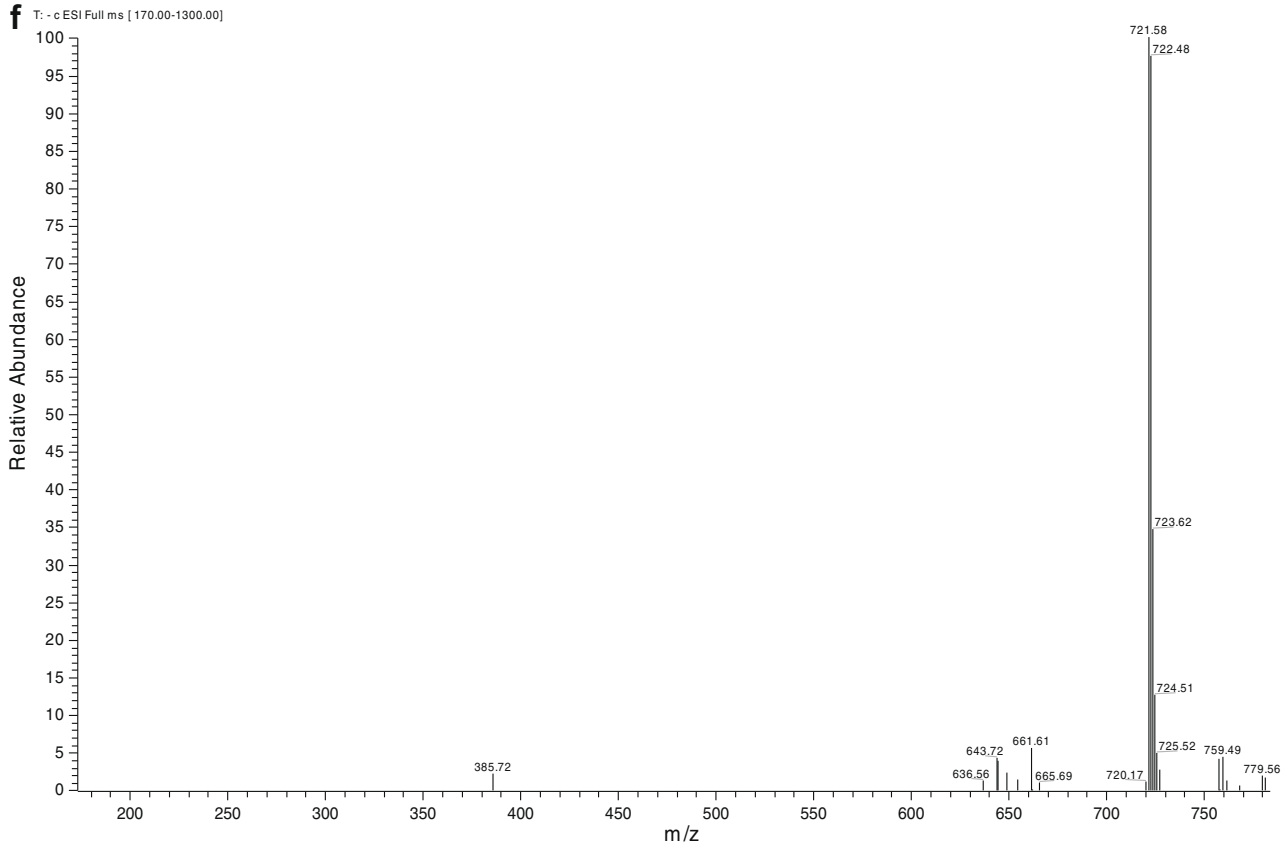

Fig. 3 (*continued*)

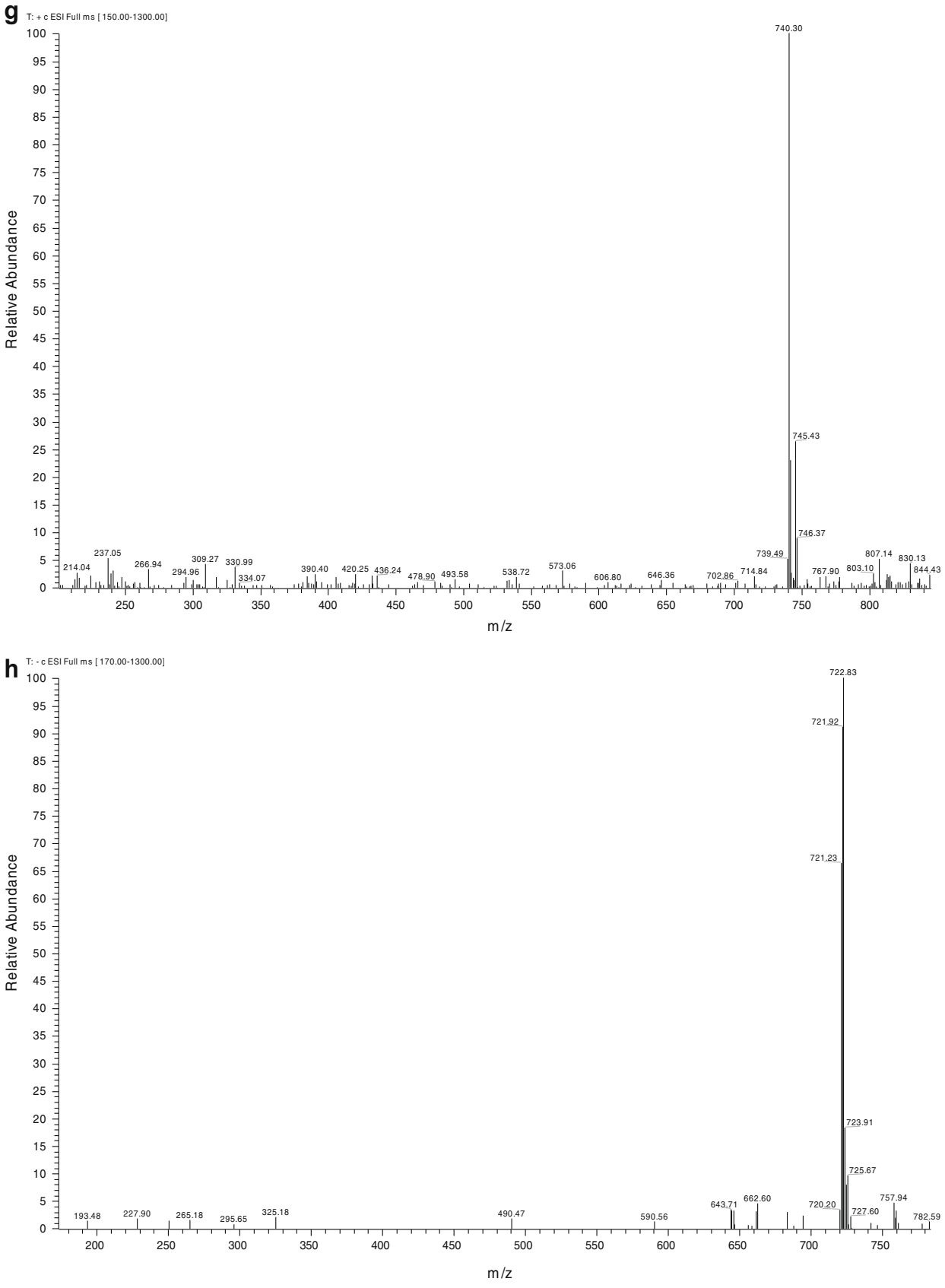

Fig. 3 (*continued*)

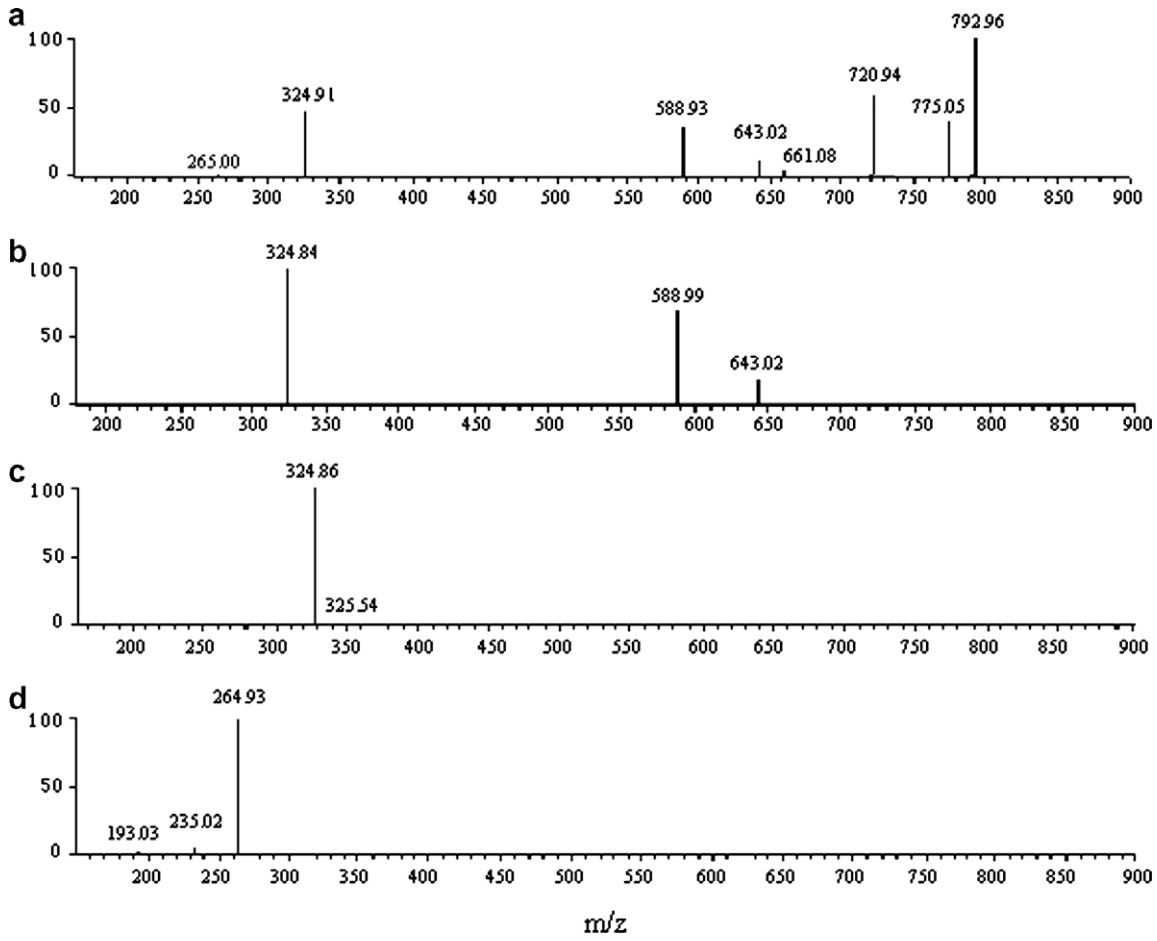

Fig. 4. MS^n spectra of a deprotonated molecule $[M-H]^-$ ion at *m/z* 853 of compound **1**. (a) MS^2 spectrum of the *m/z* 853 ion ($[M-H]^-$); (b) MS^3 spectrum of the *m/z* 721 ion from the *m/z* 853 ion ($[M-H]^-$) (853 > 721 >); (c) MS^3 spectrum of the *m/z* 589 ion from the *m/z* 853 ion ($[M-H]^-$) (853 > 589 >); and (d) MS^3 spectrum of the *m/z* 325 ion from the *m/z* 853 ion ($[M-H]^-$) (853 > 325 >).

and so on, as shown in Fig. 4a. This is similar to the cleavage mechanism of oligosaccharides in negative mode observed by Pfenninger et al. (2002a, 2002b). An ion at *m/z* 793 with loss of 60 Da ($C_2H_4O_2$) and an ion at *m/z* 661 with loss of one xylosyl residue unit and 60 Da ($C_2H_4O_2$) from the parent ion, respectively, resulted from xylosyl cross-ring cleavages. They were assigned to the $^{0,2}A$ fragment ion. Both ions at *m/z* 775 and 643 might be due to water loss from the ions at *m/z* 793 and *m/z* 661, respectively. It has been reported that the losses of 60 and 78 Da resulting from cross-ring cleavage indicate that both of the sugar units are linked by typical β-(1,4) glycosidic bonds (Garozzo et al., 1990; Pfenninger, 2002b). Both of the fragment ions at *m/z* 793 and 775, with loss of 60 and 78 Da from the parent ion at *m/z* 853, respectively, confirmed that both of the xylosyl residues from the reducing end were linked by β-(1,4) linkage. A fragment ion at *m/z* 721 (loss of 132 Da from the parent ion), corresponding to a fragment ion resulting from the loss of one xylosyl residue unit, was produced. Therefore, the reducing xylosyl residue is not substituted by another group unit. A fragment ion at *m/z* 589 with loss of two xylosyl residue units from the parent ion was detected. The fragment ion at *m/z* 325 with loss of four xylosyl residue units from the parent ion was assigned to the $C_{1\alpha}$ fragment ion, which was the molecular mass of the arabinosyl feruloylated derivative residue.

MS^3 analysis of the C_3 ion (*m/z* 853 > 721>) provides several fragment ions as shown in Fig. 4b. An ion at *m/z* 643 with losses of 60 Da ($C_2H_4O_2$) and one water molecule from the C_3 ion at *m/z* 721 indicated that the second xylosyl residue from the reducing end was linked with the third xylosyl residue by β-(1,4) glycosidic bond. A fragment ion at *m/z* 589 (loss of 132 Da), corresponding to a fragment ion resulting from the loss of one xylosyl residue unit from the C_3 ion at *m/z* 721, was assigned to C_2 fragment ion. Therefore, the second xylosyl residue from the reducing end is not substituted by another group unit. The fragment ion at *m/z* 325 with loss of three xylosyl residue units (396 Da) from the C_3 ion at *m/z* 721 was assigned to the $C_{1\alpha}$ fragment ion, which was the molecular mass of the arabinosyl feruloylated derivative residue.

MS^3 analysis of the C_2 ion (*m/z* 853 > 589 >) provides several fragment ions as shown in Fig. 4c. The fragment ion at *m/z* 325 with loss of two xylosyl residue units (264 Da) from the C_2 ion at *m/z* 589 was assigned to the $C_{1\alpha}$ fragment ion, which was the mass of the arabinosyl feruloylated derivative residue. It has been reported that the branched (1,3) linkages in underivatised oligosaccharides became relatively unstable in ESI-MS^n, if the deprotonated reducing end, including deprotonated C-fragment ions, was located at the monosaccharide subunit which contained the branching site (Pfenninger et al., 2002b). The fragment ion at *m/z* 325 was detected in MS^2 of the ion at *m/z* 853, MS^3 of the C_3 ion (*m/z* 853 > 721 >) and C_2 ion (*m/z* 853 > 589 >), demonstrating that the ion resulted from the cleavage of the branching residues. A C_1 fragment ion at *m/z* 457 should be detected if the branching residue was linked to the first xylosyl residue from the non-reducing end. In fact, such a C_1 fragment ion at *m/z* 457 was not observed. This demonstrated that the branching residue resulting in the

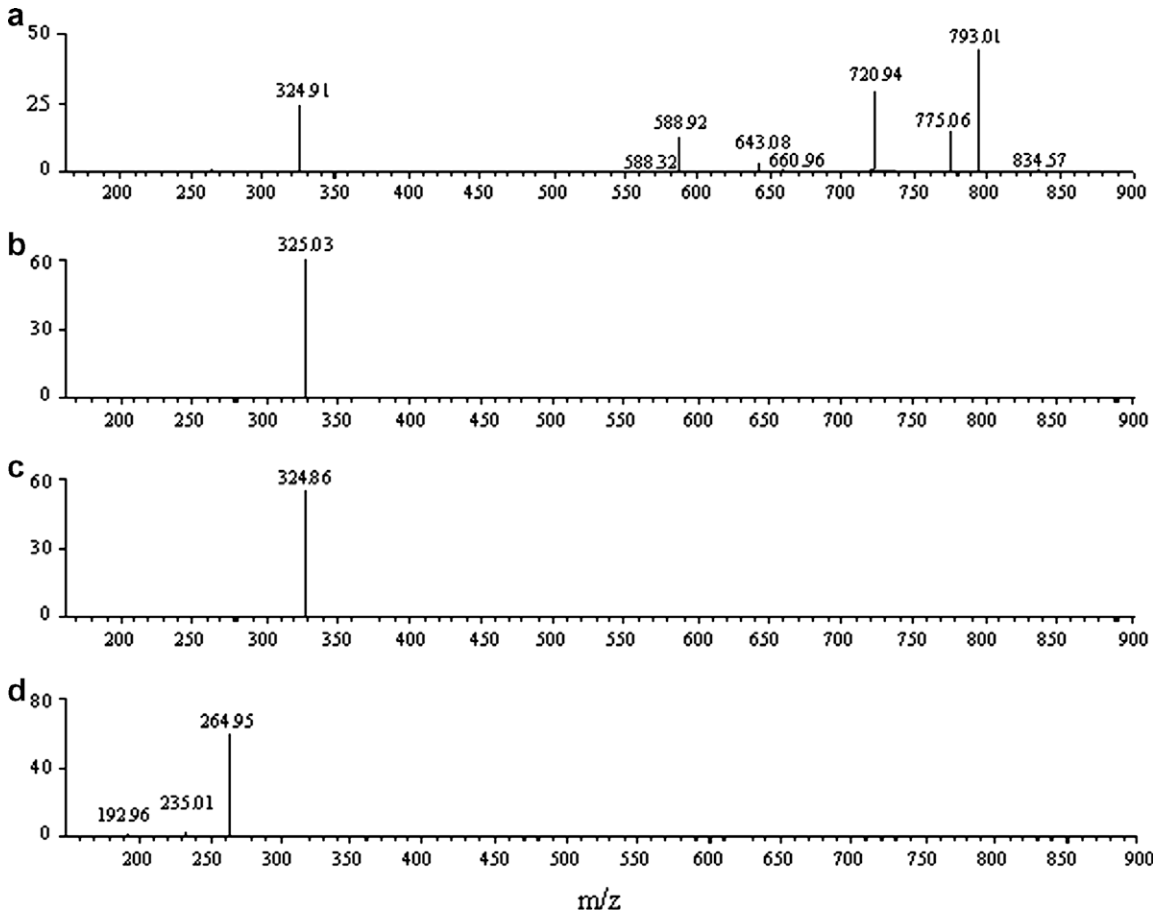

Fig. 5. MS^n spectra of a deprotonated molecule $[M-H]^-$ ion at *m/z* 853 of compound **2**. (a) MS^2 spectrum of the *m/z* 853 ion ($[M-H]^-$); (b) MS^3 spectrum of the *m/z* 721 ion from the *m/z* 853 ion ($[M-H]^-$) (853 > 721 >); (c) MS^3 spectrum of the *m/z* 589 ion from the *m/z* 853 ion ($[M-H]^-$) (853 > 589 >); and (d) MS^3 spectrum of the *m/z* 325 ion from the *m/z* 853 ion ($[M-H]^-$) (853 > 325 >).

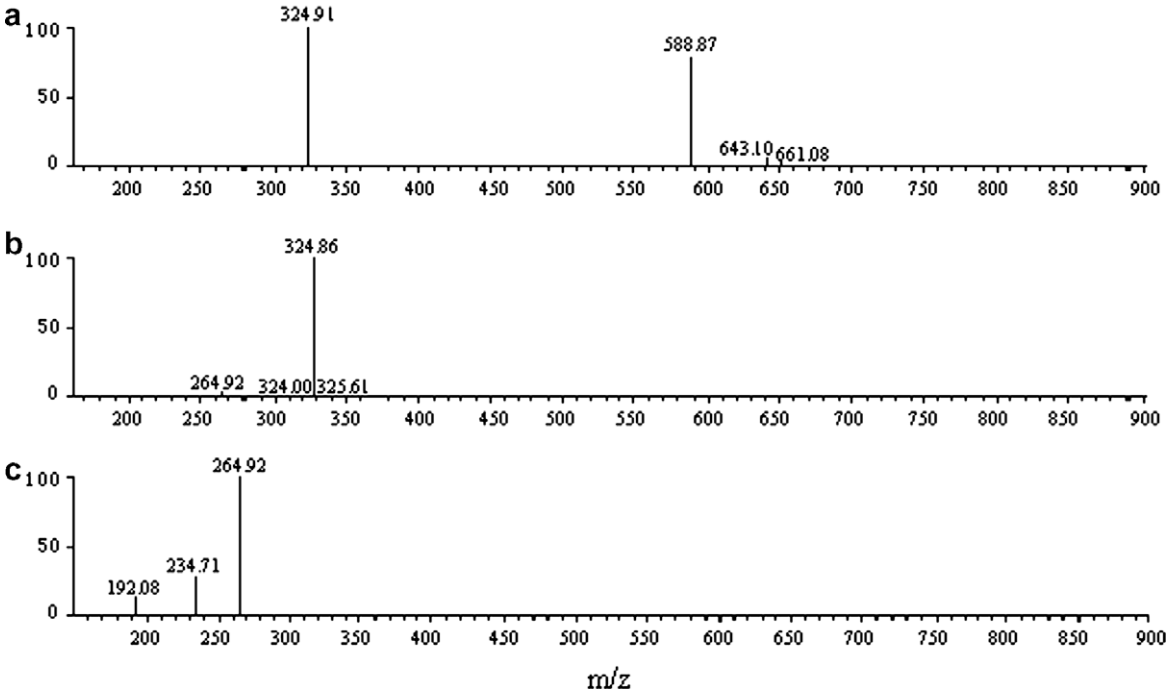

Fig. 6. MS^n spectra of a deprotonated molecule $[M-H]^-$ ion at *m/z* 721 of compound **3**. (a) MS^2 spectrum of the *m/z* 721 ion ($[M-H]^-$); (b) MS^3 spectrum of the *m/z* 589 ion from the *m/z* 721 ion ($[M-H]^-$) (721 > 589 >); (c) MS^3 spectrum of the *m/z* 325 ion from the *m/z* 721 ion ($[M-H]^-$) (721 > 325 >).

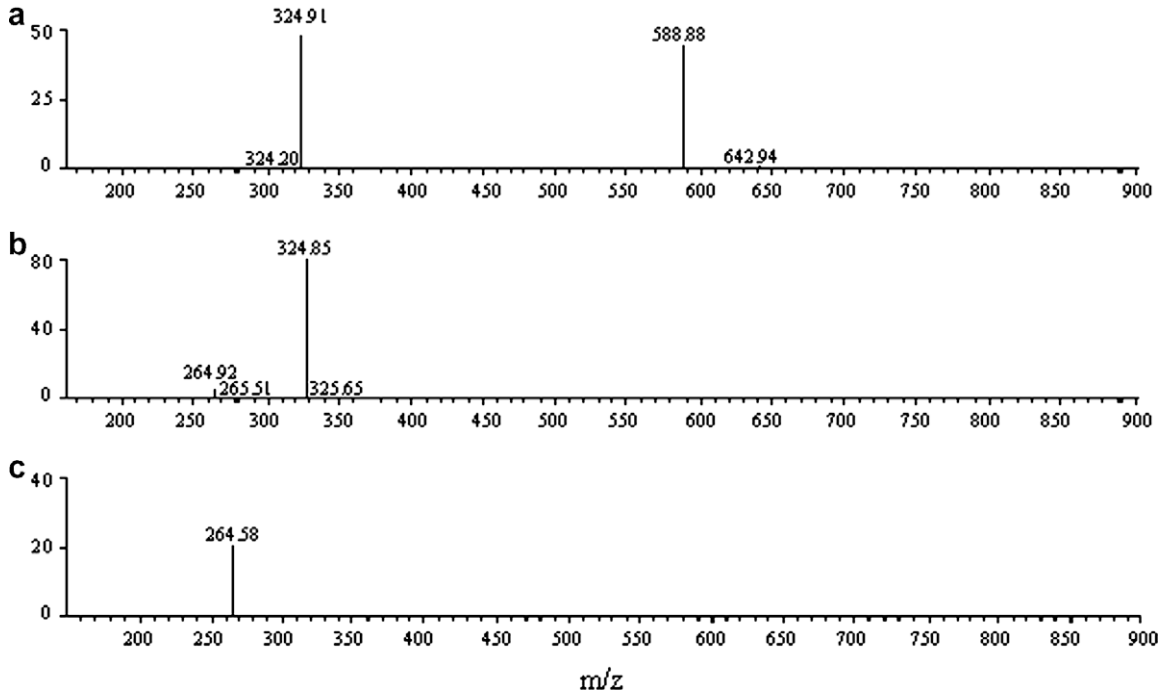

Fig. 7. MS^n spectra of a deprotonated molecule $[M-H]^-$ ion at *m/z* 721 of compound **4**. (a) MS^2 spectrum of the *m/z* 721 ion ($[M-H]^-$); (b) MS^3 spectrum of the *m/z* 589 ion from the *m/z* 721 ion ($[M-H]^-$) (721 > 589 >); (c) MS^3 spectrum of the *m/z* 325 ion from the *m/z* 721 ion ($[M-H]^-$) (721 > 325 >).

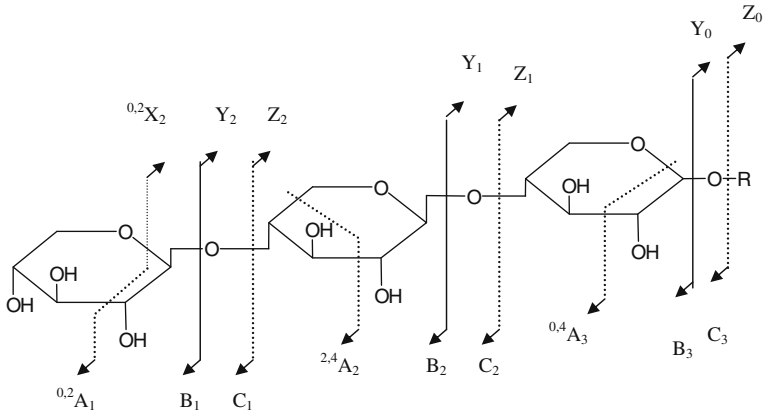

Fig. 8. Nomenclature of fragment ions from carbohydrates, according to Domon and Costello.

fragment ion at *m/z* 325 was possibly attached at the third xylosyl residue from the reducing end.

MS^3 analysis of the $C_{1\alpha}$ ion (*m/z* 853 > 325 >) provides several fragment ions, as shown in Fig. 4d. The fragment ions at *m/z* 265 and 235 with loss of 60 Da ($C_2H_4O_2$) and 90 Da ($C_3H_6O_3$) from the $C_{1\alpha}$ ion, respectively, which resulted from the cross-ring cleavage of arabinofuranose, were assigned to ^{0,2}A and ^{0,3}A ions, respectively. It has been reported that none of the saccharides linked by α-glycosidic bonds in infrared laser desorption mass spectrometry showed any peaks, due to the losses of water from the parent molecule or from a fragment; in contrast, all of the β-linked saccharides showed one or more additional peaks due to the loss of water (Spengler, Dolce, & Cotter, 1990). The fragment ion with loss of one water molecule from the $C_{1\alpha}$ ion (*m/z* 853 > 325 >) was absent in its MS^3 spectrum, which demonstrated that the arabinofuranose residue was attached to the backbone of the oligosaccharide by an α-(1,3) glycosidic linkage. In the abovementioned FT-IR spectrum of FOs, the arabinofuranose residue was linked at the position of *O*-3 in the xylopyranose. The fragment ion at *m/z* 193 with loss of one arabinofuranose residue unit (132 Da) from the $C_{1\alpha}$ ion at *m/z* 325 is the molecular mass of ferulic acid, revealing that ferulic acid is located on the *O*-5 position of the arabinofuranosyl residue (Levigne et al., 2004). Therefore, the proposed structure of compound **1** is assigned to *O*-β-D-xylopyranosyl-(1 → 4)-*O*-[5-*O*-(feruloyl)-α-L-arabinofuranosyl-(1 → 3)]- *O*-β-D-xylo-pyranosyl-(1 → 4)-*O*-β-D-xylopyranosyl-(1 → 4)-D-xylopyranose (Fig. 9a). Fig. 5 shows the MS^n spectra of a deprotonated molecule $[M-H]^-$ ion at *m/z* 853 of compound **2** at the retention time of 12.77 min. Its MS fragmentation pattern is similar to that of compound **1** by comparing MS^n spectra of their deprotonated molecular ion at *m/z* 853. The molecular mass of compounds **1** and **2** is 854 Da. These results indicate that compound **2** is an isomer of compound **1**. Compound **1** has been determined using 2D-NMR spectroscopy, and the ^{1}H NMR spectrum of the compound shows that ferulic acid is present as a *trans/cis* mixture in a ratio of 3:1 (Lequart et al., 1999). The relative large proportion of the *cis* isomer

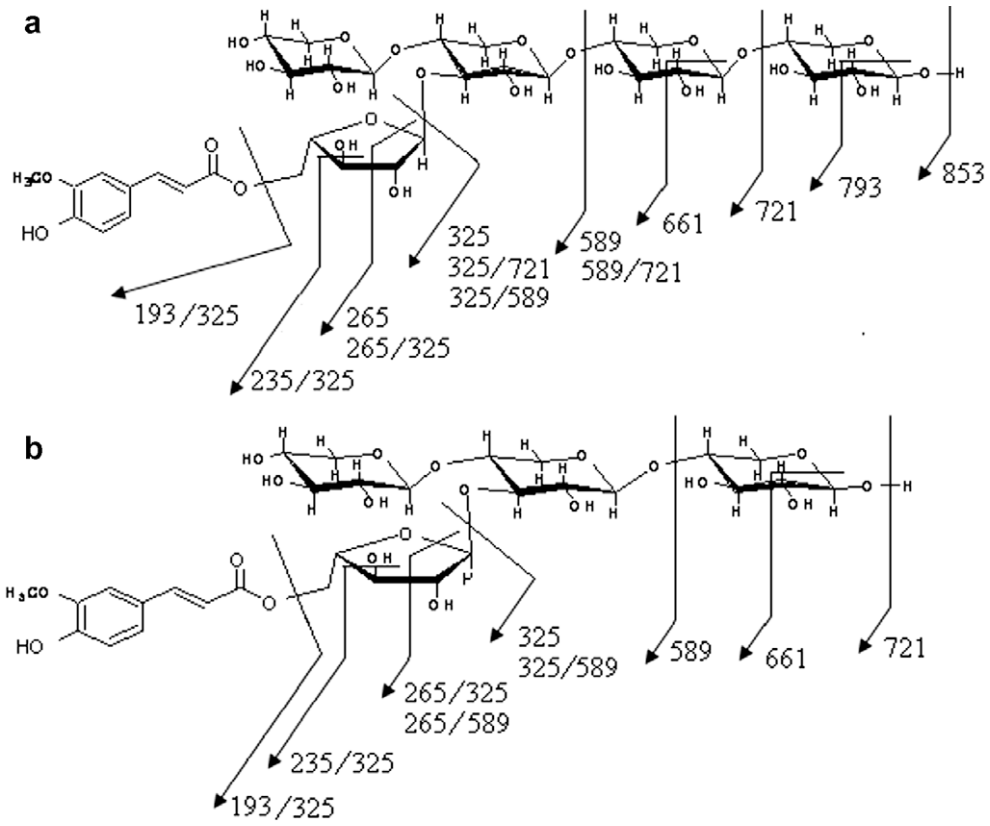

Fig. 9. (a) Proposed structure of compound **1** and observed cleavages and (b) proposed structure of compound **3** and observed cleavages.

is rather perplexing, but may suggest that this isomer is already present in significant proportion in the original plant material (Lequart et al., 1999). Further, it is reasonable to conclude that ferulic acid moieties of compounds **1** and **2** are present as *trans*- and *cis*-ferulic acid, respectively.

*3.3.2. Identification compounds **3** and **4***

Fig. 9b shows the proposed structure of compound **3** and the different cleavages observed. After collision-induced dissociation of the parent ion at *m/z* 721, the glycosidic bond and sugar ring were cleaved to form A and C type fragment ions, including mainly *m/z* 661 ($^{0,2}A_3$), 643, 589 (C_2), 325 ($C_{1\alpha}$) and so on, as shown in Fig. 6a. This is similar to the cleavage mechanism of oligosaccharides in negative mode observed by Pfenninger et al. (2002a, 2002b). An ion at *m/z* 661 with loss of 60 Da ($C_2H_4O_2$) from the parent ion resulted from xylosyl cross-ring cleavage. It was assigned to the ^{0,2}A fragment ion. The ion at *m/z* 643 may be because of water loss from the ion at *m/z* 661. Both of the fragment ions at *m/z* 661 and 643 with loss of 60 and 78D from the parent ion at *m/z* 721, respectively, confirmed that both of the xylosyl residues from the reducing end were linked by a β-(1,4) linkage. A fragment ion at *m/z* 589 (loss of 132 Da from the parent ion), corresponding to a fragment ion resulting from the loss of one xylosyl residue units, was produced. Therefore, the reducing xylosyl residue is not substituted by other group unit. The fragment ion at *m/z* 325 with loss of three xylosyl residue units from the parent ion was assigned to the $C_{1\alpha}$ fragment ion, which was the molecular mass of the arabinosyl feruloylated derivative residue.

MS^3 analysis of the C_2 ion (*m/z* 721 > 589 >) provides several fragment ions, as shown in Fig. 6b. The fragment ion at *m/z* 325 with loss of two xylosyl residue units (264 Da) from the C_2 ion was assigned to the $C_{1\alpha}$ fragment ion, which was the molecular mass of the arabinosyl feruloylated derivative residue. As for compound **1**, the fragment ion at *m/z* 325 was detected in MS^2 of the ion at *m/z* 721 and MS^3 of the C_2 ion (*m/z* 721 > 589 >), demonstrating that the ion resulted from the cleavage of the branching residues. A C_1 fragment ion at *m/z* 457 should be detected if the branching residue was linked to the first xylosyl residue from the non-reducing end. In fact, such a C_1 fragment ion at *m/z* 457 was not observed. This demonstrated that the branching residue resulting in the fragment ion at *m/z* 325 was possibly attached at the second xylosyl residue from the reducing end.

MS^3 analysis of the $C_{1\alpha}$ ion (*m/z* 721 > 325 >) provides several fragment ions as shown in Fig. 6c. The fragment ions at *m/z* 265 and 235 with loss of 60 Da ($C_2H_4O_2$) and 90 Da ($C_3H_6O_3$) from the $C_{1\alpha}$ ion, respectively, which resulted from the cross-ring cleavage of arabinofuranose, were assigned to ^{0,2}A and ^{0,3}A ions, respectively. A fragment ion with loss of one water molecule from the $C_{1\alpha}$ ion (*m/z* 721 > 325 >) was absent in its MS^3 spectrum, which demonstrated that the arabinofuranose residue was attached to the backbone of the oligosaccharide by α-(1,3) glycosidic linkage. The fragment ion at *m/z* 193 with loss of one arabinofuranose residue unit (132 Da) from the $C_{1\alpha}$ ion at *m/z* 325 is the molecular mass of ferulic acid, revealing that ferulic acid is located on the *O*-5 position of the arabinofuranosyl residue (Levigne et al., 2004). Therefore, the proposed structure of compound **3** is assigned to *O*-β-D-xylopyranosyl-(1 → 4)-*O*-[5-*O*-(feruloyl)-α-L-arabinofuranosyl-(1 → 3)]-*O*-β-D-xylopyranosyl-(1 → 4)-D-xylo-pyranose (Fig. 6b), which is similar to that isolated from the enzymatic production of wheat bran by Lequart et al. (1999). Fig. 7 shows the MS^n spectra of a deprotonated molecule $[M-H]^-$ ion at *m/z* 721of compound **4** at the retention time of 14.81 min. Its MS fragmentation pattern is similar to that of compound **3,** by comparing MS^n spectra of their deprotonated molecular ion at *m/z* 721, and the molecular mass of compounds **3** and **4** is 722 Da, indicating that compound **4** is an isomer of compound **3**. Further, like compounds **1** and **2**, it can be drawn that ferulic acid moieties of compounds **3** and **4** are present as *trans*- and *cis*-ferulic acid, respectively.

4. Conclusions

It has been demonstrated that on-line HPLC-ESI-MS^n is a fast, effective and practical tool to characterise the structure of wheat bran FOs. The molecular ion of four components of FOs shows the characteristic mass spectrometry behaviour. In negative ion mode, deprotonated ion $[M-H]^-$ yields C type of fragment ions, providing the information of the primary sequence and branching in the isolated compounds from FOs, and cross-ring A type of ions, providing the information of linkages between sugar residues.

Acknowledgements

This work was supported by Funding Project for Academic Human Resources Development in Institutions of Higher Learning and the Jurisdiction of Beijing Municipality and General Project of Beijing Municipal Education Commission.

References

Bahmed, K., Quilès, F., Bonaly, R., & Coulon, J. (2003). Florescence and infrared spectrometric study of cell walls from *Candida*, *Kluyveromyces*, *Rhodotorula* and *Schizosaccharomyces* yeasts in relation with their chemical composition. *Biomacromolecules, 4*, 1763–1772.

Benamrouche, S., Crônier, D., Debeirem, P., & Chabbertm, B. (2002). A chemical and histological study on the effect of endo-xyanase treatment on wheat bran. *Journal of Cereal Science, 36*, 253–260.

Bonaccorsi, P., Caristi, C., Gargiulli, C., & Leuzzi, U. (2008). Flavonol glucosides in *Allium* species: A comparative study by means of HPLC-DAD-ESI-MS–MS. *Food Chemistry, 107*, 1668–1673.

Broberg, A. (2007). High-performance liquid chromatography/electrospray ionization ion-trap mass spectrometry for analysis of oligosaccharides derivatized by reductive amination and N,N-dimethylation. *Carbohydrate Research, 342*, 1462–1469.

Chai, W., Piskarev, V., & Lawson, A. M. (2001). Negative-ion electrospray mass spectrometry of netural underivatized oligosaccharides. *Analytical Chemistry, 73*, 651–657.

Chaikumpollert, O., Methacanon, P., & Suchiva, K. (2004). Structural elucidation of hemicelluloses from Vetiver grass. *Carbohydrate Polymer, 57*, 191–196.

Dobhal, M. P., Hasan, A. M., Sharma, M. C., & Joshi, B. C. (1999). Ferulic acid esters from *Plumeria bicolor*. *Phytochemistry, 51*, 319–321.

Domon, B., & Costello, C. (1988). A systematic nomenclature for carbohydrate fragmentations in FAB-MS/MS spectra of glycoconjugates. *Glycoconjugate Journal, 5*, 397–409.

Garozzo, D., Giuffrida, M., & Impallomeni, G. (1990). Determination of linkage position and identification of the reducing end in linear oligosaccharides by negative ion fast atom bombardment mass spectrometry. *Analytical Chemistry, 62*, 279–286.

Geng, P., Qiu, F., Zhu, Y., & Bai, G. (2008). Four acarviosin-containing oligosaccharides identified form *Streptomyces coelicoflavus* ZG0656 are potent inhibitors of α-amylase. *Carbohydrate Research, 343*, 882–892.

Ishii, T. (1997). Structure and functions of feruloylated polysaccharides. *Plant Science, 127*, 111–127.

Kačuráková, M., Belton, P. S., Wilson, R. H., Hirsch, J., & Ebringerová, A. (1998). Hydration properties of xylan-type structures: An FTIR study of xylooligosaccharides. *Journal of the Science Food and Agriculture, 77*, 38–44.

Kačuráková, M., Capeka, P., Sasinková, V., Wellner, N., & Ebringerová, A. (2000). FT-IR study of plant cell wall model compounds: Pectic polysaccharides and hemicelluoses. *Carbohydrate Polymers, 43*, 195–203.

Katapodis, P., Vardakou, M., Kalogeris, M., Kekos, D., Macris, B. J., & Christakopoulos, P. (2003). Enzymic production of a feruloylated oligosaccharide with antioxidant activity from wheat flour arabinoxylan. *European Journal of Nutrition, 42*, 55–60.

Lequart, C., Nuzillard, J. M., Kurek, B., & Debeire, P. (1999). Hydrolysis of wheat bran and straw by an endoxylanase: Production and structural characterization of cinnamoyl-oligosaccharides. *Carbohydrate Research, 319*, 102–111.

Levigne, S. V., Ralet, M. C. J., Quéméner, B. C., Pollet, B. N. L., Lapierre, C., & Thibault, J. F. C. (2004). Isolation from sugar beet cell walls of arabinan oligosaccharides esterified by two ferulic acid monomers. *Plant Physiology, 134*, 1173–1180.

Liu, Y., Urgaonkar, S., Verkade, J. G., & Armstrong, D. W. (2005). Separation and characterization of underivatized oligosaccharides using liquid chromatography and liquid chromatography–electrospray ionization mass spectrometry. *Journal of Chromatography A, 1079*, 146–152.

McCallum, J. A., Taylor, I. E. P., & Neil Towers, G. H. (1991). Spectrophotometric assay and electrophoretic detection of *trans*-feruloyl esterase activity. *Analytical Biochemistry, 196*, 360–366.

Nandini, C. D., & Salimath, P. V. (2001). Structural features of arabinoxylans from sorghum having good *roti*-making quality. *Food Chemistry, 74*, 417–422.

Ohta, T., Yamasaki, T., Egashira, Y., & Sanada, H. (1994). Antioxidative activity of corn bran hemicellulose fragments. *Journal of Agricultural and Food Chemistry, 42*, 653–656.

Ou, S. Y., Jackson, M., Jiao, X., Chen, J., Wu, J. Z., & Huang, X. S. (2007). Protection against oxidative stress in diabetic rats by wheat bran feruloyl oligosaccharides. *Journal of Agriculture and Food Chemistry, 55*, 3191–3195.

Pfenninger, A., Karas, M., Finke, B., & Stahl, B. (2002a). Structural analysis of underivatized neutral human milk oligosaccharides in the negative ion mode by nano-electrospray MS^n (Part 1: Methodology). *Journal of the American Society for Mass Spectrometry, 13*, 1331–1340.

Pfenninger, A., Karas, M., Finke, B., & Stahl, B. (2002b). Structural analysis of underivatized neutral human milk oligosaccharides in the negative ion mode by nano-electrospray MS^n (Part 2: Application to isomeric mixtures). *Journal of the American Society for Mass Spectrometry, 13*, 1341–1348.

Quéméner, B., Ordaz-Ortiz, J. J., & Saulnier, L. (2006). Structural characterization of underivatized arabino-xylo-oligosaccharides by negative-ion electrospray mass spectrometry. *Carbohydrate Research, 341*, 1834–1847.

Rhodes, D. I., Sadek, M., & Stone, B. A. (2002). Hydroxycinnamic acids in walls of wheat aleurone cells. *Journal of Cereal Science, 36*, 67–81.

Saad, O. M., & Leary, J. A. (2005). Heparin sequencing using enzymatic digestion and ESI-MS^n with HOST: A heparin/HS oligosaccharide sequencing tool. *Analytical Chemistry, 77*, 5902–5911.

Smith, M. M., & Hartley, R. D. (1983). Occurrence and nature of ferulic acid substitution of cell-wall polysaccharides in graminaceous plants. *Carbohydrate Research, 118*, 65–80.

Spengler, B., Dolce, J. W., & Cotter, R. J. (1990). Infrared laser desorption mass spectrometry of oligosaccharides: Fragmentation mechanisms and isomer analysis. *Analytical Chemistry, 62*, 1731–1737.

Vafiadi, C., Topakas, E., Bakx, E. J., Schols, H. A., & Christakopoulos, P. (2007). Structural characterization by ESI-MS of feruloylated arabino-oligosaccharides synthesized by chemoenzymatic esterification. *Molecules, 12*, 1367–1375.

Yoshida-Shimokawa, T., Yoshida, S., Kakegawa, K., & Ishii, T. (2001). Enzymic feruloylation of arabinoxylan-trisaccharide by feruloyl-CoA: Arabinoxylan-trisaccharide *O*-hydroxycinnamoyl transferase from *Oryza sativa*. *Planta, 212*, 470–474.

Yuan, X., Wang, J., & Yao, H. (2005). Feruloyl oligosaccharides stimulate the growth of *Bifidobacterium bifidum*. *Anaerobe, 11*, 225–229.

Yuan, X., Wang, J., Yao, H., & Chen, F. (2005). Free radical-scavenging capacity and inhibitory activity on rat erythrocyte hemolysis of feruloyl oligosaccharides from wheat bran insoluble dietary fiber. *Lebensmittel-Wissenschaft und-Technologie/Food Science and Technology, 38*, 877–883.